Vibration analysis of a rotating variable thickness bladed disk for aircraft gas turbine engine using generalized differential quadrature method

B Shahriari[1], Mohammadhadi Jalali[2] and MR Karamooz Ravari[3]

Abstract

In this paper, free vibration analysis of rotating variable thickness annular bladed disk suitable to be used in aircraft gas turbine engine is investigated. The numerical generalized differential quadrature method is introduced in this paper as a fast and efficient numerical method to be used for vibration analysis of bladed disks of real gas turbine engines. The boundary conditions are supposed to be similar to those of the real bladed disk used in the aircraft engines i.e. clamped for the inner edge and free for the outer edge. Considering the thickness of the disk to vary as a power function and the blades of the bladed disk to be rigid, the numerical solution is performed and the effects of thickness variation, geometric parameters, angular velocity, and number of blades on the natural frequencies and critical speeds are investigated. The obtained numerical results are compared with those reported in the literature indicating a good agreement.

Introduction

Rotating bladed disks are one of the most fundamental components of engineering devices such as aero-gas turbine engines. An undesired vibration of these rotating systems in the operating conditions may cause catastrophic failures of the parts or even the whole engine. According to what is mentioned above, a careful design of the rotating systems is of crucial importance.

The dynamic characteristics of circular disks have been studied for several decades. Lamb et al.[1] investigated the vibration of spinning uniform disk, for the first time. They obtained an exact solution for natural frequencies of rotating, homogenous, constant thickness circular disk. Southwell[2] extended the Lamb's work and analyzed the effects of rotation on the vibration of uniform homogeneous circular disk, more deeply. Deshpande et al.[3] presented a model for in-plane vibration of rotating thin disk accounting for the stiffening of the disk due to the radial expansion resulting from its rotation. Considering that the thickness of the plate to be varied linearly and exponentially, Lee et al.[4] used the assumed modes method to formulate the equations of motion of rotating homogeneous circular annular plates. They obtained the natural frequencies and critical speeds for

vibration modes consisting of radial nodal lines without any nodal circle. Al-bedoor[5] presented a dynamic model for a typical elastic blade attached to a disk driven by a shaft, which is flexible in torsion. He employed the Lagrangian approach in conjunction with the finite element method in deriving the equations of motion, within the assumption of small deformation theory. Yang and Huang[6] studied the effects of disk flexibility, blade's stagger angle, and rotational speed on the natural frequencies and mode shapes of a shaft–disk–blade system. They derived the equations of motion using energy approach in conjunction with the assumed modes method. Yang and Huang[7] analyzed the dynamic behavior of a coupled

[1]Department of Mechanical and Aerospace Engineering, Malek-Ashtar University of Technology, Iran
[2]Department of Mechanical Engineering, Isfahan University of Technology, Isfahan, Iran
[3]Department of Mechanical Engineering, Graduate University of Advanced Technology, Kerman, Iran

Corresponding author:
B Shahriari, Department of Mechanical and Aerospace Engineering, Malek-Ashtar University of Technology, Isfahan, P.O. 83145-115, Iran.
Email: shahriari@mut-es.ac.ir

shaft–disk–blade system. They found out that the flexibility of the disk evolves the blade–blade modes into disk–blade and blade–blade modes, and causes frequency loci veering and merging with rotation. Jalali et al.[8] investigated the dynamic behavior of a rotor-bearing system by the use of experimental measurements and one-dimensional and three-dimensional finite element models. Callioglu et al.[9] studied the stress in uniform functionally graded (FG) rotating disks, numerically and analytically. They used finite element method to obtain the radial and circumferential stresses and radial displacement of rotating FG disks and compared the numerical results with the analytical ones. Kermani et al.[10] used differential quadrature method (DQM) to solve the equations of motion of rotating FG circular annular plates. They assumed that the variation of the elastic modulus and density of the plate to be an exponential function of radius and the thickness of the plate to be uniform. They investigated the natural frequencies and critical speeds of the plates with clamped–clamped (C–C), clamped–simply supported (C–S), and clamped–free (C–F) boundary conditions and they evaluated the effects of the graded index, angular velocity, and geometric parameters on the modal response. Gutzwiller et al.[11,12] developed a computer software for automated design optimization of rotating bladed disks. Using finite difference method, they obtained stresses and displacements considering various thickness variations of the plate.

In the past few years, DQM has been applied extensively for solving engineering problems. This method provides a global approach to numerical discretization, which approximates the derivatives by a linear weighted sum of all the functional values in the whole domain. Shu[13] discussed the mathematical fundamentals, recent developments, major applications in engineering, and implementation procedure of DQM. Comparing to the other numerical methods, the DQM can lead to almost accurate results using a considerably smaller number of grid points and hence requiring relatively little computational effort.[13–19] The generalized differential quadrature method (GDQM) is an improvement of the DQM especially for solving higher order differential equations, which is more computationally efficient and accurate.[20] Unlike the DQM, the GDQM considers a general situation, where the derivatives of a function are approximated using a linear weighted sum of all the functional values and also some derivatives of the functional values.[20]

To the best of the authors' knowledge, the vibration analysis of a real bladed disk using the GDQM has not been investigated until now. In this paper, free vibration of a variable thickness elastic disk with attached rigid blades is investigated using the GDQM as a fast and accurate numerical method. The boundary conditions of the disk are assumed to be clamped in the inner edge and free in the outer edge which are similar to those of real gas turbine engines. In the real aero engine, the inner edge of the bladed disk is clamped to the rotor's shaft and the outer edge of the bladed disk is free. Also, the thickness of the bladed disk is assumed to vary by a power function, which is a good and applicable approximation for the thickness variation of industrial bladed disks. The obtained results are compared with those reported in the literature, which shows good agreement. In addition, the convergence analysis is performed and the effects of the disk thickness variation, angular velocity, geometric parameters, and the number of the blades on the natural frequencies and critical speeds are investigated.

Theoretical foundation

Governing equations

A circular annular plate with outer radius a, inner radius b, thickness t, and outer surface thickness h_0, which is rotating with angular velocity $\tilde{\omega}$ is shown in Figure 1. The thickness, t, can be variable in the radial direction.

Considering the variable thickness and the plane stress formulation, the equilibrium equation in the radial direction is as follows[11]

$$\frac{\mathrm{d}}{\mathrm{d}r}(tr\sigma_r) - t\sigma_\theta + t\rho\,\tilde{\omega}^2\,r^2 = 0 \tag{1}$$

where σ_r is the radial stress, σ_θ the circumferential stress, and ρ the density. Application of the axisymmetric assumption ($\frac{\partial}{\partial\theta} = 0$) to the Kirshoff's strain–displacement relations leads to the following[11]

$$\varepsilon_r = \frac{\mathrm{d}u}{\mathrm{d}r}, \quad \varepsilon_\theta = \frac{u}{r}, \quad \gamma_{r\theta} = 0 \tag{2}$$

where u is the radial displacement. The stress–strain relations, i.e. the Hook's law is given by[11]

$$\sigma_r = \frac{E}{1-\upsilon^2}(\varepsilon_r + \upsilon\varepsilon_\theta), \quad \sigma_\theta = \frac{E}{1-\upsilon^2}(\upsilon\varepsilon_r + \varepsilon_\theta) \tag{3}$$
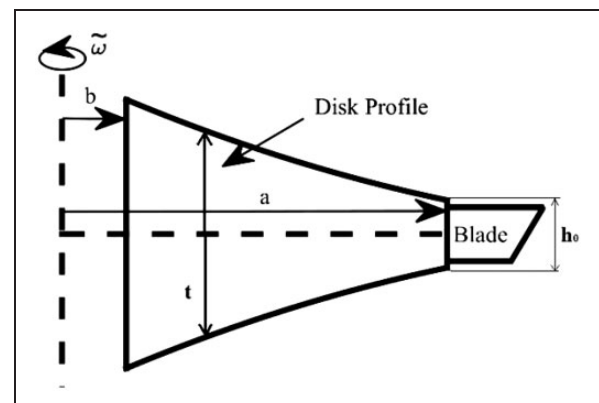
Figure 1. Rotating annular plate.

where E is the Young's modulus and υ the Poisson's ratio, which is assumed to be constant. By substituting equation (2) into equation (3), stresses are obtained in terms of radial displacement as[11]

$$\sigma_r = \frac{E}{1-\upsilon^2}\left(\frac{du}{dr} + \frac{\upsilon u}{r}\right), \quad \sigma_\theta = \frac{E}{1-\upsilon^2}\left(\frac{\upsilon du}{dr} + \frac{u}{r}\right) \quad (4)$$

By substituting equation (4) into equation (1), the equilibrium equation is obtained in terms of radial displacement. To be able to solve the obtained equation, it is necessary to apply the boundary conditions. In this paper, it is supposed that the inner edge of the disk is clamped while the outer one is free. Accordingly, the radial displacement of the inner edge must be set to zero and in the outer edge, the radial stress should be equal to the stress produced by the centrifugal force of the blades. The equation below shows the mathematical description of these boundary conditions[11]

$$@\,r = b, \quad u = 0 \quad \text{and} \quad @\,r = a, \quad \sigma_r = \frac{n_b m_b r_{cg}\tilde{\omega}^2}{2\pi r h_0} \quad (5)$$

where n_b is the number of blades, m_b is the mass of each blade, and r_{cg} is the radius of the center of the mass of each blade.

Governing equations for vibration analysis

The governing equation for out-of-plane vibration of a rotating disk of variable thickness and variable material properties can be expressed as[21]

$$D\nabla^4 w + \frac{dD}{dr}\left[2\frac{\partial}{\partial r}(\nabla^2 w) + \frac{1}{r}\left(\upsilon\frac{\partial^2 w}{\partial r^2} + \frac{1}{r}\frac{\partial w}{\partial r} + \frac{1}{r^2}\frac{\partial^2 w}{\partial\theta^2}\right)\right]$$
$$+ \frac{d^2 D}{dr^2}\left[\frac{\partial^2 w}{\partial r^2} + \upsilon\left(\frac{1}{r}\frac{\partial w}{\partial r} + \frac{1}{r^2}\frac{\partial^2 w}{\partial\theta^2}\right)\right]$$
$$- \frac{1}{r}\frac{\partial}{\partial r}\left(tr\sigma_r\frac{\partial w}{\partial r}\right) - \frac{1}{r^2}t\sigma_\theta\frac{\partial^2 w}{\partial\theta^2} + \rho t\frac{\partial^2 w}{\partial t^2} = 0 \quad (6)$$

where w is the out-of-plane deflection, $D = \frac{Et^3}{12(1-\upsilon^2)}$ the flexural rigidity of the disk, $\nabla^2 = \frac{\partial^2}{\partial r^2} + \left(\frac{1}{r}\right)\frac{\partial}{\partial r} + \frac{1}{r^2}\frac{\partial^2}{\partial\theta^2}$ the Laplacian operator. The thickness of the disk is assumed to vary in the radial direction by the following equation

$$t = h_0\left(\frac{r}{a}\right)^{m_1} \quad (7)$$

where m_1 is a constant. Once again, the C–F boundary condition must be applied which

$$@\,r = b, \quad w = 0, \quad \frac{\partial w}{\partial r} = 0 \quad (8)$$

$$@\,r = a, \quad M_r = -D\left[\frac{\partial^2 w}{\partial r^2} + \upsilon\left(\frac{1}{r}\frac{\partial w}{\partial r} + \frac{1}{r^2}\frac{\partial^2 w}{\partial\theta^2}\right)\right] = 0,$$
$$V_r = -D\left[\frac{\partial^3 w}{\partial r^3} + \frac{1}{r^2}\frac{\partial^2 w}{\partial r^2} - \frac{1}{r^2}\frac{\partial w}{\partial r} + \frac{2-\upsilon}{r^2}\frac{\partial^3 w}{\partial r\partial\theta^2} - \frac{3-\upsilon}{r^3}\frac{\partial^2 w}{\partial\theta^2}\right]$$
$$- \frac{dD}{dr}\left[\frac{\partial^2 w}{\partial r^2} + \upsilon\left(\frac{1}{r}\frac{\partial w}{\partial r} + \frac{1}{r^2}\frac{\partial^2 w}{\partial\theta^2}\right)\right] = 0 \quad (9)$$

The out-of-plane deflection, w, may be written as

$$w = W(r)\cos(m\theta)e^{i\omega t} \quad (10)$$

where m is the angular wave number, and ω the natural frequency. By substituting equations (7), (4), and (10) into equation (6), the following governing equation in terms of $W(r)$ is obtained

$$r^{2m_1}\frac{d^4 W}{dr^4} + P_1\frac{d^3 W}{dr^3} + P_2\frac{d^2 W}{dr^2} + P_3\frac{dW}{dr} + P_4 W = 0 \quad (11)$$

Where

$$P_1 = 2r^{2m_1-1}(3m_1 + 1)$$
$$P_2 = r^{2m_1-2}(-1 + 3m_1(1 + \upsilon + 3m_1) - 2m^2)$$
$$\quad - \frac{12a^{2m_1}}{h_0^2}\left(\frac{du}{dr} + \frac{\upsilon u}{r}\right)$$
$$P_3 = r^{2m_1-3}\left((3m_1 - 1)(-1 + 3\upsilon m_1 - 2m^2)\right) - \frac{12a^{2m_1}}{h_0^2}$$
$$\quad \times \left((1 + m_1)\left(\frac{1}{r}\frac{du}{dr} + \frac{\upsilon u}{r^2}\right) + \frac{d^2 u}{dr^2} - \frac{\upsilon u}{r^2} + \frac{\upsilon}{r}\frac{du}{dr}\right)$$
$$P_4 = r^{2m_1-4}\left(m^4 - m^2(4 + 3m_1(-3 + \upsilon(3m_1 - 1)))\right)$$
$$\quad + \frac{12m^2 a^{2m_1}}{h_0^2 r^2}\left(\frac{\upsilon du}{dr} + \frac{u}{r}\right) - \frac{12\rho(1 - \upsilon^2)a^{2m_1}}{Eh_0^2}\omega^2$$

Substituting equation (10) into equations (8) and (9), the boundary conditions can be expressed as follows

$$@\,r = b, \quad W = 0, \quad \frac{dW}{dr} = 0$$
$$@\,r = a, \quad \frac{d^2 W}{dr^2} + \upsilon\left(\frac{1}{r}\frac{dW}{dr} - \frac{m^2}{r^2}W\right) = 0$$
$$@\,r = a, \quad \frac{d^3 W}{dr^3} + \frac{1 + 3m_1}{r}\frac{d^2 W}{dr^2}$$
$$\quad + \left[\frac{-1 - m^2(2 - \upsilon) + 3m_1\upsilon}{r^2}\right]\frac{dW}{dr}$$
$$\quad + \left[\frac{m^2(3 - \upsilon) - 3m_1 m^2\upsilon}{r^2}\right]W = 0 \quad (12)$$

By introducing the dimensionless parameters, $R = \frac{r}{a}$, $\bar{W} = \frac{W}{h_0}$, $\bar{u} = \frac{u}{h_0}$, and $\Omega = \frac{\omega a^2}{h_0}\sqrt{\frac{12\rho(1-\upsilon^2)}{E}}$ the governing equation and boundary conditions can be

expressed using equations (13) and (14), respectively

$$R^{2m_1}\frac{d^4\bar{W}}{dR^4} + \bar{P}_1\frac{d^3\bar{W}}{dR^3} + \bar{P}_2\frac{d^2\bar{W}}{dR^2} + \bar{P}_3\frac{d\bar{W}}{dR} + \bar{P}_4\bar{W} = 0$$

(13)

$$@R = b/a, \quad \bar{W} = 0, \quad \frac{d\bar{W}}{dR} = 0$$

$$@R = 1, \quad \frac{d^2\bar{W}}{dR^2} + \upsilon\left(\frac{1}{R}\frac{d\bar{W}}{dR} - \frac{m^2}{R^2}\bar{W}\right) = 0$$

$$@R = 1, \quad \frac{d^3\bar{W}}{dR^3} + \frac{1+3m_1}{R}\frac{d^2\bar{W}}{dR^2}$$

(14)

$$+ \left[\frac{-1 - m^2(2-\upsilon) + 3m_1\upsilon}{R^2}\right]\frac{d\bar{W}}{dR}$$

$$+ \left[\frac{m^2(3-\upsilon) - 3m_1\upsilon m^2}{R^3}\right]\bar{W} = 0$$

where

$$\bar{P}_1 = 2R^{2m_1-2}(3m_1 - 1)$$

$$\bar{P}_2 = R^{2m_1-2}\big(-1 + (3m_1)(1 + \upsilon + 3m_1) - 2m^2\big)$$

$$\quad - \frac{12a}{h_0}\left(\frac{d\bar{u}}{dR} + \frac{\upsilon\bar{u}}{R}\right)$$

$$\bar{P}_3 = R^{2m_1-3}\big((3m_1 - 1)(-1 + 3\upsilon m_1 - 2m^2)\big) - \frac{12a}{h_0}$$

$$\quad \times \left((1 + m_1)\left(\frac{1}{R}\frac{d\bar{u}}{dR} + \frac{\upsilon}{R^2}\bar{u}\right) + \frac{d^2\bar{u}}{dR^2} - \frac{\upsilon\bar{u}}{R^2} + \frac{\upsilon}{R}\frac{d\bar{u}}{dR}\right)$$

$$\bar{P}_4 = R^{2m_1-4}\big(m^4 - m^2(4 + (3m_1)(-3 + \upsilon(3m_1 - 1)))\big)$$

$$\quad + \frac{12m^2a}{h_0 R^2}\left(\frac{\upsilon d\bar{u}}{dR} + \frac{\bar{u}}{R}\right) - \Omega^2$$

In order to solve the governing equation presented as equation (13) and to obtain the dimensionless natural frequency (Ω), the GDQM is used. In the following subsection, this method is briefly explained.

Generalized differential quadrature method

In the numerical GDQ method, the solution domain is divided into points R_i ($i = 1, 2,..., N$) and the derivatives of a function with the weighted summation of that function.[20] The GDQR expression for a fourth-order boundary value differential equation may be expressed as follows[20]

$$\bar{W}^{(S)}(R_i) = \frac{d^s\bar{W}(R_i)}{dR^s} = \sum_{j=1}^{N+2} E_{ij}^{(S)}U_j \quad i = 1, 2, \ldots, N$$

(14)

where $\{U_1, U_2, .., U_{N+2}\} = \left\{\bar{W}_1, \bar{W}_1^{(1)}, \bar{W}_2, \ldots, \bar{W}_N, \bar{W}_N^{(1)}\right\}$,

$\bar{W}_j$ is the function value at j-th point, $\bar{W}_1^{(1)}$ and $\bar{W}_N^{(1)}$ are the first-order derivatives of the dimensionless displacement function at the first and N-th points, respectively. $E_{ij}^{(S)}$ are the S-order weighting coefficients at points R_i. The GDQR explicit weighting

coefficients have been derived in Sadasue et al.[22] and Chao and Qi[23] and are used directly in this paper.

In order to discretize the solution space, two discretization schemes namely, (I) equally spaced points and (II) Chebyshev–Gauss–Lobatlo discretization, are used in this paper. The second discretization method can be formulated as

$$R_i = \frac{1}{a}\left[\frac{1}{2}\left[1 - \text{Cos}\frac{(i-1)\pi}{N-1}\right](a-b) + b\right] \quad i = 1, 2, \ldots, N$$

(15)

Appling GDQM to equation (13) yields the following governing equation[20]

$$H_{ij}U_j = \Omega^2\bar{W}_i \quad i = 2, 3, \ldots, N-1$$

(16)

in which H_{ij} is a $(N) \times (N+2)$ matrix. Adding four boundary conditions to the above $(N-2)$ equations leads to $(N+2)$ algebraic equations, which can be arranged as[20]

$$\begin{bmatrix} [S_{bb}] & [S_{bd}] \\ [S_{db}] & [S_{dd}] \end{bmatrix}\begin{bmatrix} U_b \\ U_d \end{bmatrix} = \begin{bmatrix} 0 \\ \omega^2 U_d \end{bmatrix}$$

(17)

where

$$U_b = \begin{bmatrix} \bar{W}_1 \\ \bar{W}_1^{(1)} \\ \bar{W}_N \\ \bar{W}_N^{(1)} \end{bmatrix}, \quad U_d = \begin{bmatrix} \bar{W}_2 \\ \vdots \\ \bar{W}_{N-1} \end{bmatrix}$$

By matrix sub-structuring and manipulation, one obtains a standard eigenvalue problem as follows[20]

$$[S]U_d = \Omega^2 U_d$$

(18)

in which $[S] = [S_{dd}] - [S_{db}][S_{bb}]^{-1}[S_{bd}]$ is a $(N-2) \times (N-2)$ matrix. The dimensionless natural frequency (Ω) can be obtained by solving the eigenvalue problem of equation (18).

Application of boundary conditions in GDQM

The following equations are the GDQ form of the C–F boundary conditions:

$$\bar{W}_1 = 0, \quad U_1 = 0$$

$$\bar{W}_1^{(1)} = 0, \quad U_2 = 0$$

$$\sum_{j=1}^{N+2} E_{Nj}^{(2)}U_j + \frac{\upsilon}{R_N}\bar{W}_N^{(1)} - \frac{\upsilon m^2}{R_N^2}\bar{W}_N = 0$$

$$\sum_{j=1}^{N+2} E_{Nj}^{(3)}U_j + \frac{1+3m_1}{R_N}\sum_{j=1}^{N+2} E_{Nj}^{(2)}U_j$$

$$+ \left[\frac{-1 - m^2(2 - \upsilon) + 3m_1\upsilon}{R_N^2} \right] \bar{W}_N^{(1)}$$

$$+ \left[\frac{m^2(3 - \upsilon) - 3m_1\upsilon m^2}{R_N^3} \right] \bar{W}_N = 0 \qquad (19)$$

By separating the boundary and domain coefficients in equation (16), one would have

$$H_{i1} U_1 + H_{i2} U_2 + H_{iN+1} U_{N+1} + H_{iN+2} U_{N+2}$$
$$+ \sum_{j=3}^{N} H_{ij} U_j = \Omega^2 \bar{W}_i \quad i = 2, \ldots, N - 1 \qquad (20)$$

By separating the boundary and domain coefficients in equation (19) and using equation (20), the following sub-matrices are obtained.

$$S_{bb} = \begin{bmatrix} 1 & 0 & 0 & 0 \\ 0 & 1 & 0 & 0 \\ E_{N1}^{(2)} & E_{N2}^{(2)} & E_{NN+1}^{(2)} - \frac{\upsilon m^2}{R_N^2} & E_{NN+2}^{(2)} + \frac{\upsilon}{R_N} \\ S_{bb1} & S_{bb2} & S_{bb3} & S_{bb4} \end{bmatrix}$$
$$(21)$$

where

$$S_{bb1} = E_{N_1}^{(3)} + \frac{1 + 3m_1}{R_N} E_{N1}^{(2)}$$

$$S_{bb2} = E_{N_2}^{(3)} + \frac{1 + 3m_1}{R_N} E_{N_2}^{(2)}$$

$$S_{bb3} = E_{NN+1}^{(3)} + \frac{1 + 3m_1}{R_N} E_{NN+1}^{(2)}$$
$$+ \frac{m^2(3 - \upsilon) - 3m_1 m^2 \upsilon}{R_N^3}$$

$$S_{bb4} = E_{NN+2}^{(3)} + \frac{1 + 3m_1}{R_N} E_{NN+2}^{(2)}$$
$$+ \frac{-1 - m^2(2 - \upsilon) + 3m_1\upsilon}{R_N^2}$$

$$S_{bd} = \begin{bmatrix} [0]_{2*4} \\ S_{bd3} \\ S_{bd4} \end{bmatrix}$$

$$S_{db} = \begin{bmatrix} H_{i1} & H_{i2} & H_{iN+1} & H_{iN+2} \end{bmatrix} \quad i = 2, \ldots, N - 1$$
$$S_{dd} = H_{ij} \quad i = 2, \ldots, N - 1, \quad j = 3, \ldots, N$$

in which $S_{bd3} = E_{Nj}^{(2)}$, $j = 3, \ldots, N$, and $S_{bd4} = E_{Nj}^{(3)} + \frac{1+3m_1}{R_N} E_{Nj}^{(2)}, j = 3, \ldots, N$. By obtaining the dimensionless natural frequency (Ω), the natural frequency (ω) can be calculated. Note that the obtained natural frequency is the natural frequency in the rotating (noninertial) coordinate system, which is attached to the rotating plate. For each ω in the rotating coordinate system, there would be two corresponding natural frequencies in the stationary (inertial) coordinate system. These natural frequencies are obtained as[10]

$$\omega^f = \omega + m\tilde{\omega} \qquad (22)$$

$$\omega^b = \omega - m\tilde{\omega} \qquad (23)$$

Table 1. Properties of the bladed disk.

Parameter	E (GPa)	ρ (kg/m^3)	υ	r_{cg} (cm)	m_b (g)
Value	380	3800	0.3	9	6
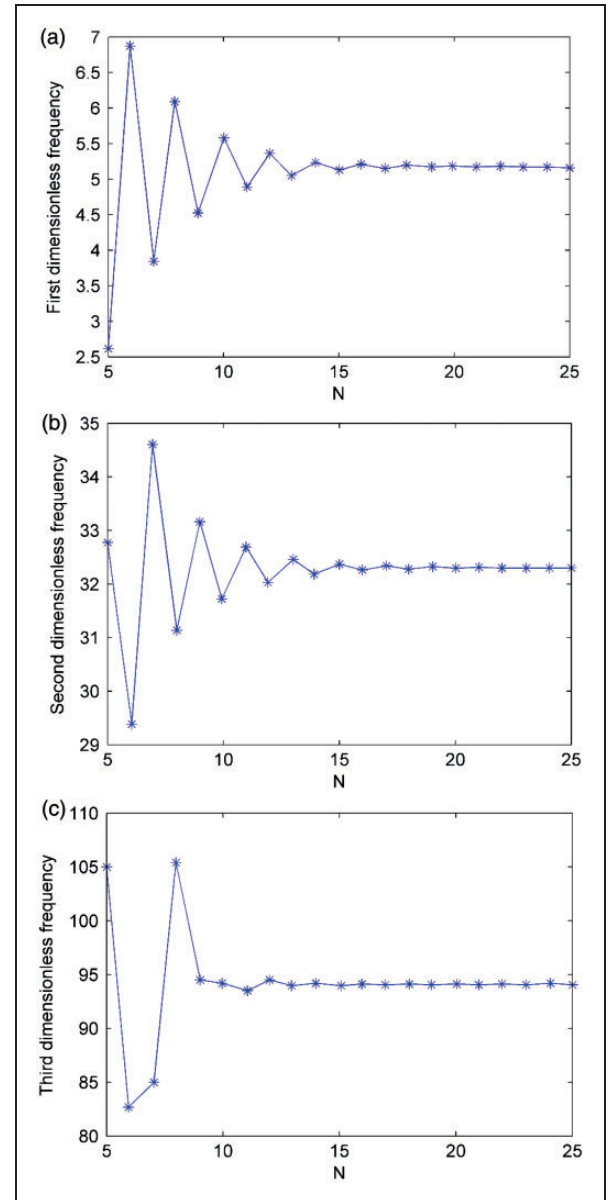
Figure 2. Discretization method (I) convergence diagram of (a) first, (b) second, (c) third dimensionless frequency.
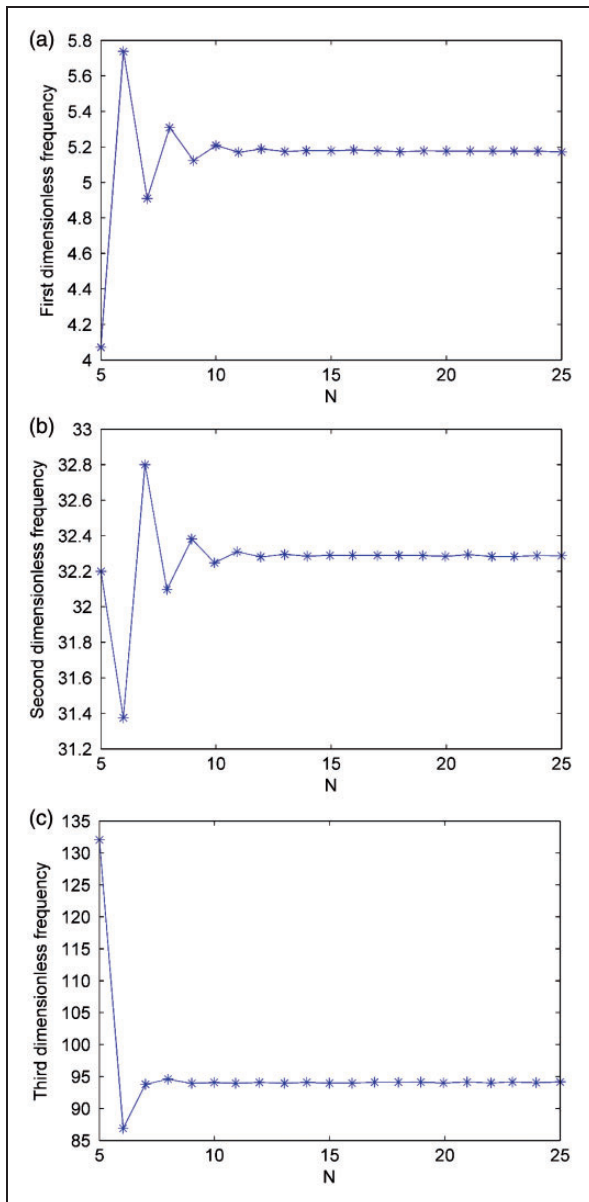
Figure 3. Discretization method (II) convergence diagram of (a) first, (b) second, (c) third dimensionless frequency.

where ω^f and ω^b are the forward and backward natural frequencies, respectively. Whenever ω^b is equal to zero, the critical speed might occur.

Numerical results

A MATLAB program is developed to calculate the dimensionless natural frequency. In this section, first, the convergence of the proposed method is assessed for both utilized schemes. Then, the presented approach is validated against previously reported numerical results.

Convergence analysis

For the sake of numerical implementation, the parameters presented in Table 1 are utilized.

As mentioned earlier, for the discretization of the plate in the radial direction, two discretization methods, denoted as (I) and (II) are used. Figure 2 shows the convergence diagram for the first three dimensionless natural frequencies using method (I). As can be seen from the figure, by increasing the number of points, N, the variation in the results decreases. For the values greater than 15, this variation is negligible. Figure 3 shows the same diagram for discretization scheme (II). It can be seen from these figures that the convergence of the method using this discretization method is guaranteed if a sufficiently high number of points is utilized.

Validation of the proposed approach

Tables 2 and 3 compare the first dimensionless natural frequencies of the homogeneous disk without blades obtained using the proposed method with those reported in Kermani et al.[10] The data presented in the former table are obtained using the discretization scheme (I) while those reported in the latter table are obtained using scheme (II). Referring to these two tables, it can be concluded that the convergence of

Table 2. The first dimensionless natural frequency of a disk without bade for different values of wave number obtained using the discretization method (I) ($m_1 = 0$, $h_0/a = 0.001$, $b/a = 0.2$).

m	0	1	2	3	4	5
Present $N = 15$	5.134	4.802	6.051	11.447	19.806	30.286
Kermani et al.[10] $N = 15$	5.172	4.694	6.030	12.097	21.316	32.907
Error %	0.73	2.30	0.34	5.37	7.08	7.96
Present $N = 20$	5.185	4.939	6.502	12.099	20.551	31.115
Kermani et al.[10] $N = 20$	5.215	4.822	6.360	12.417	21.535	33.029
Error %	0.57	2.42	2.23	2.56	4.56	5.79
Present $N = 25$	5.180	4.898	6.440	12.147	20.782	31.628
Kermani et al.[10] $N = 25$	5.180	4.817	6.342	12.394	21.514	33.014
Error %	0	1.68	1.54	1.99	3.40	4.19

Table 3. The first dimensionless natural frequency of a disk without blade for different values of wave number obtained using the discretization method (II) ($m_1 = 0$, $h_0/_a = 0.001$, $b/_a = 0.2$).

m	0	1	2	3	4	5
Present $N = 15$	5.180	5.006	6.441	11.588	19.558	29.607
Kermani et al.[10] $N = 15$	5.172	4.694	6.030	12.097	21.316	32.907
Error %	0.15	6.64	6.81	4.20	8.24	10.02
Present $N = 20$	5.181	4.959	6.447	11.861	20.316	30.661
Kermani et al.[10] $N = 20$	5.125	4.822	6.360	12.417	21.535	33.029
Error %	1.09	2.84	1.36	4.47	5.66	7.16
Present $N = 25$	5.181	4.929	6.447	12.016	20.511	31.240
Kermani et al.[10] $N = 25$	5.213	4.817	6.342	12.394	21.514	33.014
Error %	0.61	2.32	1.65	3.04	4.66	5.37
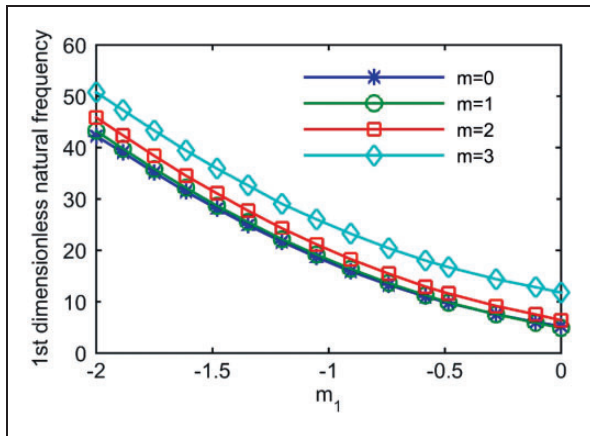
Figure 4. Variation of the first dimensionless natural frequency with the thickness variation for different values of wave number, m.
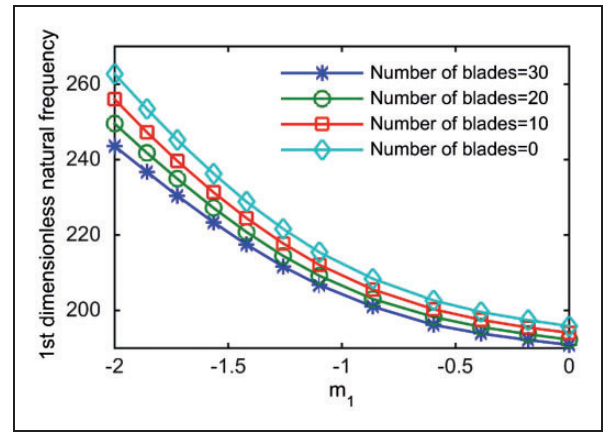
Figure 5. Variation of the first dimensionless natural frequency with the thickness variation for different number of blades (rotating speed = 10,000 r/min) ($m = 1$).

the frequency value is achieved so that increasing the value of N would not affect this value significantly. In addition, referring to the value of the error percentage presented in Tables 2 and 3, the obtained results are in good agreement with those reported in Kermani et al.[10] indicating that the proposed model can be successfully utilized for predicting the modal response of rotating variable thickness bladed disks.

Investigating effects of thickness variation and number of blades on the natural frequency

Figure 4 shows the effect of thickness variation on the first dimensionless natural frequency for different values of wave numbers, m. As can be seen, an increase in the value of m_1 from -2 to 0 decreases the first dimensionless natural frequency. It means that the constant thickness disk has the lowest first natural frequency and by using the variable thickness disk, a higher natural frequency may be obtained.

Figure 5 depicts the variation of the first dimensionless natural frequency with parameter m_1 for
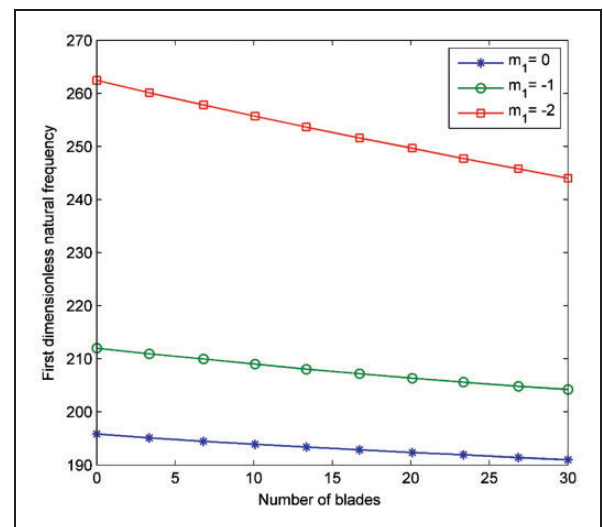
Figure 6. Variation of the first dimensionless natural frequency with the number of blades for different thickness variations (rotating speed = 10,000 r/min) ($m = 1$).

various numbers of blades. As it can be seen, by increasing the number of the blades the fundamental natural frequency decreases. In addition, it can be observed that the lowest natural frequency is related to the constant thickness disk. However, by increasing the value of m_1 from -2 to 0, which means that decreasing the amount of variation of the thickness in radial direction causes a decrease in the natural frequency. Consequently, the lowest natural frequency corresponds to a constant thickness bladed disk with the highest number of blades.

The influence of the number of blades on the fundamental natural frequency is depicted in Figure 6. Referring to this figure, increasing the number of the blades decreases the fundamental natural frequency. Also, the effect of the number of blades on

the natural frequency is more pronounced for $m_1 = -2$ and has the smallest effect for $m_1 = 0$. It means that by increasing the amount of thickness variation in a bladed disk, the influence of the number of attached blades on the modal data gets more pronounced.

Investigating the effects of angular velocity on the natural frequencies

For investigating the effects of rotating speed on the dimensionless natural frequencies, a disk without blade with the parameters of $m_1 = -1$, $h_0/a = 0.01$, $b/a = 0.2$ is considered. Figures 7 to 9 show the variation of the first three dimensionless forward and backward natural frequencies with rotating speeds
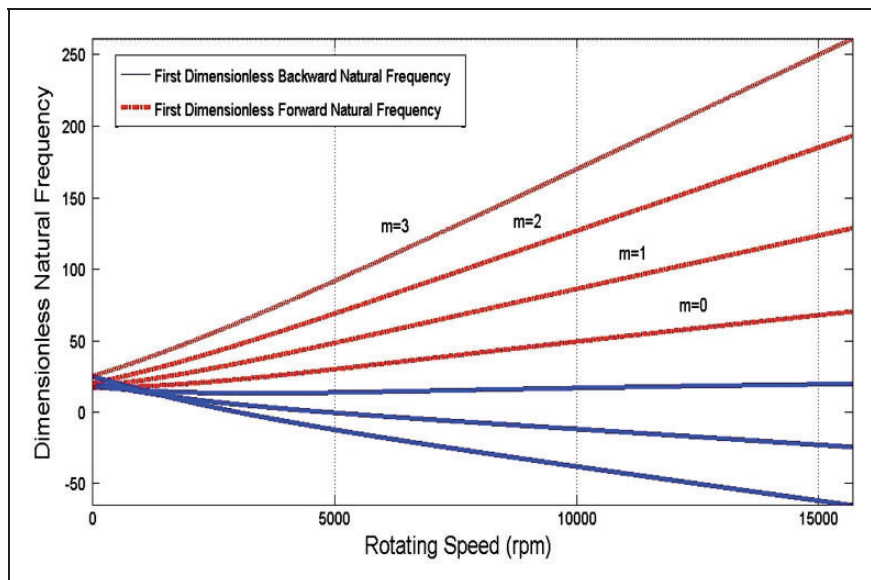
Figure 7. The variation of the first dimensionless natural frequency with rotating speed for different values of wave number.
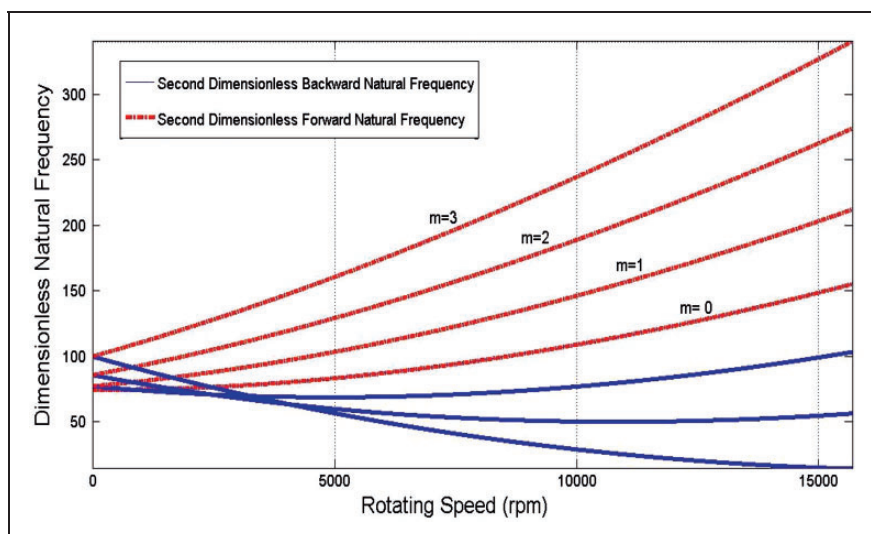
Figure 8. The variation of the second dimensionless natural frequency with rotating speed for different values of wave number.
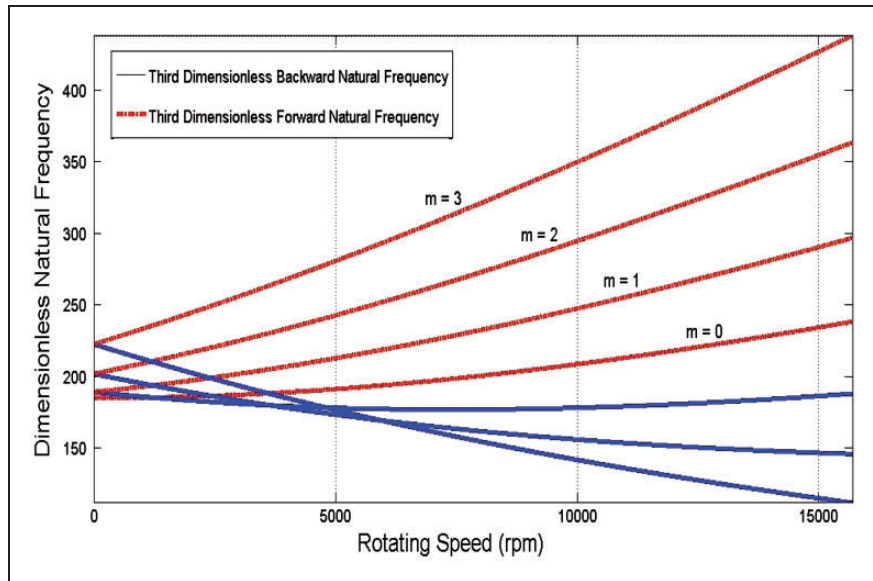
Figure 9. The variation of the third dimensionless natural frequency with rotating speed for different values of wave number.
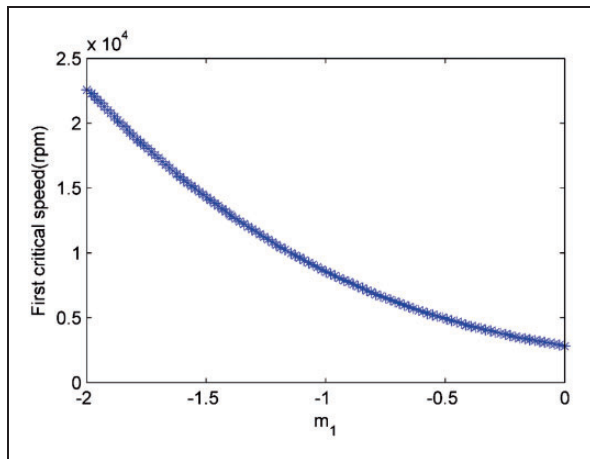
Figure 10. Variation of the first critical angular velocity with the thickness variation ($m = 2$).

Table 4. The first critical speed (r/min) for different number of blades ($m = 2$, $h_0/a = 0.01$, $b/a = 0.2$).

Number of blades	0	10	20	30	40
$m_1 = -2$	22,642	22,629	22,615	22,601	22,588
$m_1 = -1$	8511	8510	8508	8506	8505
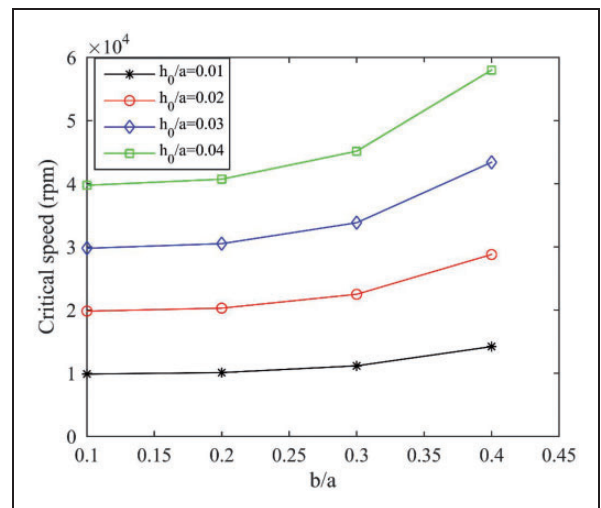
Figure 11. Variation of the critical speed with (inner radius)/ (outer radius) ratio for different values of (outer thickness)/ (outer radius) ratio ($m_1 = -1$, $m = 2$, number of blades $= 30$).

for different wave numbers, respectively. As stated before, whenever the backward natural frequency equals to zero, the critical angular velocity occurs. Figures 7 to 9 are well-known Campbell diagrams, which give valuable information for the design of any rotating machine. The intersection of the backward natural frequencies curves with the rotating speed axis gives us the rotating speed in which the backward natural frequencies equal to zero. The obtained rotating speed from this intersection is the critical speed and must be avoided in the design of bladed disks.

Investigating the effects of thickness variation and number of blades on the critical angular velocity

As mentioned earlier, whenever the backward natural frequency equals to zero, the critical angular velocity

occurs. Figure 10 shows the effect of thickness variation on the first critical speed of the bladed disk with 40 blades. As it is obvious from the figure, the constant thickness disk ($m_1 = 0$) has the lowest critical speed. In addition, by increasing the absolute value of the parameter m_1 this critical speed increases.

It shows that using variable thickness bladed disk, one can achieve higher critical speeds.

Table 4 presents the first critical speed of the rotating bladed disk with different number of blades. Referring to this table, it can be understood that the effect of number of blades on the critical speed is more pronounced when the thickness variation of the disk is more ($m_1 = -2$). It means that the variation of the first critical speed with the variation of number of blades is more for $m_1 = -2$ than for $m_1 = -1$.

Investigating the effects of the dimensionless geometrical parameters on the critical speed

In Figure 11, the effects of (inner radius)/(outer radius) ratio, b/a, and (outer thickness)/(outer radius) ratio, h_0/a, on the critical speed is shown. The trend of this plot is in good agreement with the results reported in Lee and Ng.[4] It can be seen that an increase in b/a as well as h_0/a ratio may increase the critical speed. It is worthwhile to mention that the same analyses are performed for different values of m and m_1 and the same trends are observed (not presented here for the sake of brevity).

Conclusions

Generalized differential quadrature method is utilized to investigate free vibration of variable thickness rotating bladed disks that can be used in gas turbine engines. Compared with other numerical approaches, the GDQM just needs a few number of grid points in order to achieve high-precision solutions with a good convergence rate and little computational efforts. This paper dealt with elastic disks with attached rigid blades and investigated the effects of number of the blades, geometric parameters, thickness variation, and angular velocity on the natural frequencies and critical speeds of bladed disks using GDQM. To do so, the equations of motion of the rotating variable thickness elastic disk with attached rigid blades are obtained, and the GDQM is used to discretize these equations with a relatively small number of grid points. Using this numerical method, the equations of motion are changed to an algebraic eigenvalue problem, which can be solved simply by any existing method. After analyzing the convergence of the method, the natural frequencies and critical speeds of the bladed disk are obtained and are validated against what is reported in the literature. Finally, the effects of different corresponding parameters on the natural frequencies as well as critical speeds of bladed disks are assessed and the following conclusions are made:

1. Using a constant thickness disk, a lower natural frequency and a lower critical speed can be obtained.

2. Increasing the number of the blades decreases the natural frequency and critical speed of the system.
3. The effect of the number of the blades on the modal data is more pronounced when the thickness variation of the disk is more.
4. By increasing the (inner radius)/ (outer radius) as well as (outer thickness)/ (outer radius) ratio, the critical speed increases.

References

1. Lamb H and Southwell R. The vibrations of a spinning disk. *Proc Roy Soc Lond Ser A* 1921; 99: 272–280.
2. Southwell R. On the free transverse vibrations of a uniform circular disc clamped at its centre; and on the effects of rotation. *Proc Roy Soc Lond A* 1922; 101: 133–153.
3. Deshpande M and Mote C. In-plane vibrations of a thin rotating disk. *J Vib Acoust* 2003; 125: 68–72.
4. Lee H and Ng T. Vibration and critical speeds of a spinning annular disk of varying thickness. *J Sound Vib* 1995; 187: 39–50.
5. Al-Bedoor B. Dynamic model of coupled shaft torsional and blade bending deformations in rotors. *Comput Meth Appl Mech Eng* 1999; 169: 177–190.
6. Yang C-H and Huang S-C. The influence of disk's flexibility on coupling vibration of shaft–disk–blades systems. *J Sound Vib* 2007; 301: 1–17.
7. Yang C-H and Huang S-C. Coupling vibrations in rotating shaft-disk-blades system. *J Vib Acoust* 2007; 129: 48–57.
8. Jalali MH, Ghayour M, Ziaei-Rad S, et al. Dynamic analysis of a high speed rotor-bearing system. *Measurement* 2014; 53: 1–9.
9. Çalhoğlu H, Bektaş NB and Sayer M. Stress analysis of functionally graded rotating discs: Analytical and numerical solutions. *Acta Mech Sin* 2011; 27: 950–955.
10. Kermani ID, Mirdamadi HR and Ghayour M. Nonlinear stability analysis of rotational dynamics and transversal vibrations of annular circular thin plates functionally graded in radial direction by differential quadrature. *J Vib Control* 2014; DOI: 1077546314547530.
11. Gutzwiller D. *Automated design, analysis, and optimization of turbomachinery disks*. MSc Thesis, University of Cincinnati, USA, 2009.
12. Gutzwiller DP and Turner MG. Rapid low fidelity turbomachinery disk optimization. *Adv Eng Softw* 2010; 41: 779–791.

13. Shu C. *Differential quadrature and its application in engineering*. New York: Springer Science & Business Media, 2000.

14. Aragh BS, Farahani EB and Barati AN. Natural frequency analysis of continuously graded carbon nanotube-reinforced cylindrical shells based on third-order shear deformation theory. *Math Mech Solids* 2013; 18: 264–284.

15. Daneshjou K, Talebitooti M, Talebitooti R, et al. Dynamic analysis and critical speed of rotating laminated conical shells with orthogonal stiffeners using generalized differential quadrature method. *Latin Am J Solids Struct* 2013; 10: 349–390.

16. Haftchenari H, Darvizeh M, Darvizeh A, et al. Dynamic analysis of composite cylindrical shells using differential quadrature method (DQM). *Compos Struct* 2007; 78: 292–298.

17. Liew K, Ng T and Zhang JZ. Differential quadrature–layerwise modeling technique for three-dimensional analysis of cross-ply laminated plates of various edge-supports. *Comput Meth Appl Mech Eng* 2002; 191: 3811–3832.

18. Ng T, Li H and Lam K. Generalized differential quadrature for free vibration of rotating composite laminated conical shell with various boundary conditions. *Int J Mech Sci* 2003; 45: 567–587.

19. Wang X and Wang Y. Free vibration analyses of thin sector plates by the new version of differential quadrature method. *Comput Meth Appl Mech Eng* 2004; 193: 3957–3971.

20. Wu T and Liu G. The generalized differential quadrature rule for fourth-order differential equations. *Int J Numer Meth Eng* 2001; 50: 1907–1929.

21. Irie T, Yamada G and Kanda R. Free vibration of rotating non-uniform discs: Spline interpolation technique calculations. *J Sound Vib* 1979; 66: 13–23.

22. Liu G and Wu T. Vibration analysis of beams using the generalized differential quadrature rule and domain decomposition. *J Sound Vib* 2001; 246: 461–481.

23. Wu TY and Liu GR. A differential quadrature as a numerical method to solve differential equations. *Comput Mech* 1999; 24: 197–205.